Available online at www.sciencedirect.com
SCIENCE DIRECT
Surface Science 600 (2006) 2195–2206
SURFACE SCIENCE
www.elsevier.com/locate/susc

Ion fractions in the scattering of hydrogen on different reconstructed silicon surfaces

Evelina A. García [a,*], C. González Pascual [b], P.G. Bolcatto [c], M.C.G. Passeggi [a,d], E.C. Goldberg [a]

[a] Instituto de Desarrollo Tecnológico para la Industria Química (CONICET-UNL), Güemes 3450, cc91, 3000 Santa Fe, Argentina
[b] Departamento Física Teórica de la Materia Condensada, C-V, Universidad Autónoma de Madrid, Canto Blanco, E-28049, Spain
[c] Facultad de Ingeniería Química and Facultad de Humanidades y Ciencias, Universidad Nacional del Litoral, Santa Fe, Argentina
[d] Facultad de Bioquímica y Ciencias Biolólogicas, Universidad Nacional del Litoral, Santa Fe, Argentina

Received 21 October 2005; accepted for publication 10 March 2006
Available online 31 March 2006

Abstract

A theoretical calculation that accounts for a fairly complete description of the resonant charge-exchange process occurring in H^0 scattering by Si surfaces is presented. Two reconstructed surfaces for the target: Si(1 0 0)2×1 and Si(1 1 1)7×7, are analyzed in this work. The interacting system is described by an extended spin-less Anderson Hamiltonian where valence as well as core states of the surface atoms are included. The interaction terms are calculated by taking into account the extended features of the surface and the localized atom–atom interactions within a mean-field approximation. The study is focused mainly in the description of the collision process in terms of short range interactions. The density of states for the surface and subsurface atoms are obtained in each case, from a molecular dynamic-density functional theory in the local density approximation. A binary elastic collision is assumed to fix the projectile trajectory, while the inelastic processes are determined by the interaction of the projectile atom with all the surface atoms 'seen' along its trajectory. The ion fractions are calculated by using the Keldysh–Green's function formalism to solve the time dependent process. We analyze the negative ion fractions of hydrogen measured by Maazouz et al. By including the interaction of the ion projectile with the target atoms seen during its trajectory and averaging over a variety of scattering centers as it may occur in the experimental situation, we obtained a smooth dependence with the exit angle that does not reflect the specific details of the local density of states and the surface topography while reproducing very well the general trends of the experiment. The ion fraction is found to be almost independent on the incoming energy for large values of the exit angles, while in the opposite cases where the projectile spends longer times in contact with the surface, the effect of the parallel component of the velocity has an increasing importance. Thus, the fine details of the surface are 'better captured' as the parallel velocity component becomes smaller.

Keywords: Atom–solid interactions; Hydrogen; Silicon surface; Charge transfer; Green–Keldysh formalism

1. Introduction

Ion surface collisions have become an useful and reliable tool for studies and analysis of solid surfaces. For many surfaces ion scattering spectrometry (ISS) analysis is capable to discriminate contributions to the backscattering yield coming from both different atomic layers and different atoms present in the surface. The collision process occurs within a dynamical situation in which charge exchange between the projectile and the solid target evolves in time. It has been noted that neutralization of the scattered ions is strongly dependent on the projectile–target combination [1–17], this being caused by the varied characteristics of the electronic structure of both subsystems. A number

* Corresponding author.
E-mail address: egarcia@intec.unl.edu.ar (E.A. García).

0039-6028/$ - see front matter © 2006 Elsevier B.V. All rights reserved.
doi:10.1016/j.susc.2006.03.008

of experimental and theoretical studies on resonant electron transfer process have been performed for the case of metal surfaces, although not much has been done concerning with detailed studies of semiconductor ones [18–23]. A thorough investigation of this process on semiconductors characterized by the existence of a band gap and the presence of specific surfaces states, playing an important role in the reactivity of these surfaces, appears of great interest. Among various possibilities, H^+ is the simplest projectile and the understanding of its interaction with solid surfaces is one of the current topics in surface science. Indeed, protons and hydrogen play an important role not only in surface chemistry but also in plasma physics and thin-film growth [24–31]. Central to this problem is the dynamics of charge transfer, being the formation of H^- a particular case of resonant electron capture.

In ion surface collisions one usually distinguish three regimes: (i) large scattering angle that under backscattering conditions involve almost normal collisions (the scattering angle is defined as that between the exit trajectory (classical) and the direction obtained after prolonging the incoming trajectory), (ii) small scattering angle, or the grazing collisions regime, and (iii) intermediate scattering angle involving in general, non-specular collisions. The large angle regime under backscattering conditions have been analyzed for many different projectile–target combinations [1,2,32–34], and it has been found that in these cases resonant charge-transfer is an important mechanism of neutralization [5–10]. Grazing angle collisions [35,36] have been described within a semiclassical rate equation scheme to obtain the population of the projectile-state. The dependencies of the position and width of the projectile level with the distance from the surface, are used as parameters, this being based on the broadening of the electron distribution caused by the parallel component of the velocity [37,38]. Actually, the interest resides in the search for an appropriate theoretical description for collisions occurring between these two limiting conditions. As far as charge exchange is concerned, answers to how the charge state of hydrogen is determined when ejected from a solid under near grazing angle conditions, are still controversial. An attempt to clarify this point is one of the aims of the present work.

Maazouz et al. [3,39,40] have measured the H^- formation in collisions of H^- and H^+ ions of 1–4 keV against Al, Mg, Ag and Si(1 1 1)7×7 surfaces for a scattering angle of 38°, being the emerging ion fractions investigated in an range of exit angles covering from 2° to 36° with reference to the surface plane. As the measurements performed with both H^- and H^+ beams give practically the same negative ion fractions, it is concluded that the charge 'memory' of the incident ion is lost during the incoming trajectory, due to an efficient resonant neutralization. They also found that the negative ion fractions on Si are of the same magnitude as for clean metal surfaces like Al. A dynamic velocity-dependent effect in electron capture is observed, and a non-resonant velocity-dependent charge transfer process involving localized dangling bond surface states, is invoked to explain this observation.

Several theoretical approaches [38,41,42] have been applied to reproduce the experimental findings in Al. All of them use the semiclassical rate equation method accounting only for the second half of the collision process when the projectile atom (ion) leaves the surface. Thus, the 'initial' charge state adopted in this case becomes an input parameter, external to the calculation. At large values of the perpendicular component of the velocity or large exit angles, the results are different depending on the selected (H^0 or H^+) initial charge. Better agreement with experiment is obtained by assuming H^0 as the initial charge. This in turns has been discussed in terms of incoming particles colliding with surface atoms at small impact parameters and rather large exit angles. The authors argued that under such violent collisions one can expect that any H^- formed during the incoming trajectory would loose its outer electron, justifying in this form the neutral initial condition. An important conclusion from these works is that within this ample range of collision angles a better description of the surfaces including its crystallographic structure, is required. This also suggests that to account more properly for the violent collisions occurring in the process, a quantum mechanical approach to the charge transfer process should be preferable to semiclassical rate equation methods. In this direction, Merino et al. [42] have taken into account the short-range interactions in order to obtain the position and width of the projectile level along the trajectory.

In this work we present results of a theoretical investigation of H^- ions formation in collisions of 1 and 4 keV of hydrogen with a Si(1 0 0)2×1 and Si(1 1 1) 7×7 surfaces. The scattered ion fractions were investigated in a exit angular range extending from 4° to 34° with reference to the surface plane. The calculation is based on a detailed description of the interaction parameters for the system H–Si, and also by using a realistic density of states for the reconstructed surfaces obtained with the code FIREBALL96 [43]. The energy and hopping terms are obtained from a bond-pair approximation to the Hamiltonian that describes the projectile–surface interacting system [44]. As the natural reference frame is provided by the surface, the relative orientations of the projectile orbital states with reference to the surface plane cannot be ignored if one looks for a correct description of the angular dependence of the charge transfer process. We focused our study mainly on the description of the collision process in terms of short range interactions. These already provide fairly good agreement with the tendencies shown by the experiments. Thus, additional long range effects as well as those of kinematic origin caused by the introduction of translation factors, are only slightly addressed in the text and deserve further investigations. The two times Green's function technique introduced by Keldysh [45] is used to

solve the time dependent evolution of the resonant charge-exchange process. Although functions involving electronic excitations of the substrate are included in the formalism no attempts to follow and analyze separately this aspect of the problem is made here. In the description of the interacting system valence as well as the 1s, 2s and 2p core states of the surface atoms, are included. The projectile trajectories with respect to the surface are described as in a classical binary collision, with one of the atoms at the surface acting as the scatterer. In this form, the features concerning with the scattering geometry as well as with the experimental set-up to avoid for counting multiple collisions effects, are well reproduced. On the other hand, the electronic processes involve the interaction of the projectile with all sub- and surface atoms in the substrate. Although all atoms in the substrate are formally included in the calculation, the effective ones are limited up to distances beyond which the bond pair model produce negligible contributions to the effective interaction parameters. From a practical point of view, this amounts to consider in our case a near-neighbors interaction sphere with a radius up to 13 bohr centered at the projectile position in each point of its trajectory. The projectile closest distance of approach to the surface is being determined from the interaction energy of the projectile–target atom system.

We found that our results are in good agreement with the experimental ones measured by Maazouz et al. [39] for the case of negative ion formation, after an average over different possible scattering centers is performed.

This work is organized as follows: in Section 2 there is a summarized description of the theoretical aspects; Section 3 is devoted to the discussion of the results. Finally, the concluding remarks are presented in Section 4.

2. Theory

2.1. The time-dependent Hamiltonian and the ion-fraction calculation

An Anderson-like Hamiltonian in the spin-less approximation is adopted to describe the collision process. This approximation is appropriate when only one active state of the projectile can be assumed to be involved in the charge exchange process. In the case of H^+ colliding with a Si surface, the ionization level (−13.6 eV) is resonant with the valence band and practically total neutralization is expected during the incoming trajectory. By considering the energy location of the affinity level (−0.75 eV) and the energy difference with the ionization level, one expects that the spin-less approximation provides a good description of the negative ion formation by assuming an initial neutral charge state for the incoming hydrogen [46]. This is also supported by the experimental evidence that H^+ and H^- incoming projectiles lead to practically the same negative ion fractions [39].

The Hamiltonian is written as

$$H = \sum_k \epsilon_k \hat{n}_k + \sum_l \epsilon_l \hat{n}_l + E_\alpha(t)\hat{n}_\alpha + \sum_k \left[T_{k,\alpha}(t)\hat{c}_k^+ \hat{c}_\alpha + \text{h.c.}\right] + \sum_l \left[T_{l,\alpha}(t)\hat{c}_l^+ \hat{c}_\alpha + \text{h.c.}\right] \quad (1)$$

where the index α refers to the active state localized at the projectile atom with energy $E_\alpha(t)$, while the indexes k and l refer to the valence- and core-band states of the solid with energies ϵ_k and ϵ_l, respectively. $T_{k,\alpha}(t)$ and $T_{l,\alpha}(t)$ represent the corresponding hopping integrals. The core bands, assumedly formed by strongly localized states are: $l = 1s$, 2s and 2p-orbital with energies equal to −1839 eV, −149.5 eV, and −99.8 eV (with respect to the Fermi level), respectively. The time dependence of the parameters comes from the classical trajectory $\overline{R} = \overline{R}(t)$ with constant velocity v.

2.2. Quantum mechanical calculation of the ion-fraction

In the spin-less approximation $\langle \hat{n}_\alpha(t) \rangle$ gives the probability that the projectile state is occupied at time t. The other possibility is the empty state with probability given by $1 - \langle \hat{n}_\alpha(t) \rangle$. The average occupation number is obtained from the time-dependent Green's function [45]:

$$F_{\alpha\alpha}(t,t') = \mathrm{i}\langle 0 | \hat{c}_\alpha^+(t')\hat{c}_\alpha(t) - \hat{c}_\alpha(t)\hat{c}_\alpha^+(t') | 0 \rangle \quad (2)$$

thus, $\langle \hat{n}_\alpha(t) \rangle$ is given by

$$\langle \hat{n}_\alpha(t') \rangle = \frac{1}{2}[1 - \mathrm{i}F_{\alpha\alpha}(t',t')] \quad (3)$$

The function $F_{\alpha\alpha}(t,t')$ is calculated by solving its equation of motion:

$$\frac{\mathrm{d}}{\mathrm{d}t}F_{\alpha\alpha}(t,t') = \mathrm{i}\left\langle \left[\hat{c}_\alpha^+(t'), \frac{\mathrm{d}}{\mathrm{d}t}\hat{c}_\alpha(t)\right] \right\rangle = \mathrm{i}\left\langle \left[\hat{c}_\alpha^+(t'), -\mathrm{i}[H(t), \hat{c}_\alpha(t)]\right] \right\rangle \quad (4)$$

Accordingly with expression (1) for the Hamiltonian, Eq. (4) results to be:

$$\mathrm{i}\frac{\mathrm{d}}{\mathrm{d}t}F_{\alpha\alpha}(t,t') = E_\alpha(t)F_{\alpha\alpha}(t,t') + \int_{t_0}^{t} \mathrm{d}t_1 \Sigma^R(t,t_1)F_{\alpha\alpha}(t_1,t') + \int_{t_0}^{t'} \mathrm{d}t_1 \Omega(t,t_1)G^{\mathrm{A}}_{\alpha\alpha}(t_1,t') \quad (5)$$

where the last term arises from the boundary condition:

$$F_{k\alpha}(t_0,t') = (2n_k - 1)G^{\mathrm{A}}_{k\alpha}(t_0,t') \quad (6)$$

n_k being the occupation of the surface k-states at the initial time t_0, and $G^{\mathrm{A}}_{k\alpha}$ the advanced Green function defined as

$$G^{\mathrm{A}}_{k\alpha}(t,t') = \mathrm{i}\Theta(t'-t)\langle\{\hat{c}_\alpha^+(t'), \hat{c}_k(t)\}\rangle \quad (7)$$

$G^{\mathrm{A}}_{k\alpha}(t_0,t')$ is determined through its equation of motion, which in turns requires the advanced function $G^{\mathrm{A}}_{\alpha\alpha}(t,t')$.

This advanced function is obtained by solving the equation of motion:

$$\mathrm{i}\frac{\mathrm{d}}{\mathrm{d}t}G^{\mathrm{A}}_{\alpha\alpha}(t,t') = \delta(t-t') + E_\alpha(t)G^{\mathrm{A}}_{\alpha\alpha}(t,t') + \int_t^{t'} \mathrm{d}t_1 \Sigma^{\mathrm{A}}(t,t_1)G^{\mathrm{A}}_{\alpha\alpha}(t_1,t') \quad (8)$$

Eqs. (5) and (8) have to be solved with the boundary conditions:

$$G^{\mathrm{A}}_{\alpha\alpha}(t',t') = \mathrm{i} \quad (9)$$

$$F_{\alpha\alpha}(t_0,t') = (2n_\alpha(t_0)-1)G^{\mathrm{A}}_{\alpha\alpha}(t_0,t') \quad (10)$$

with the time t' fixed at value corresponding to the end of the collision process. The self-energies introduced in these equations are given by

$$\Sigma^{\mathrm{A}}(t,t_1) = \mathrm{i}\Theta(t_1-t)\sum_{K=k+l} T^*_{\alpha,K}(t)T_{K,\alpha}(t_1)\exp[-\mathrm{i}\epsilon_K(t-t_1)] \quad (11)$$

$$\Sigma^{R}(t,t_1) = \Sigma^{\mathrm{A}}(t_1,t)^* \quad (12)$$

$$\Omega(t,t_1) = -\mathrm{i}\sum_{K=k+l} T^*_{\alpha,K}(t)T_{K,\alpha}(t_1)\exp[-\mathrm{i}\epsilon_K(t-t_1)](1-2n_K) \quad (13)$$

2.3. Energy level and hopping terms calculation

The model proposed for the atom–surface interaction can be thought as a generalization of the interaction between two atoms, where one of them consist of a system having a large basis set $\{\varphi_k\}$ (including extended valence and core-like states) [44]. The description is based on the symmetric orthogonalization procedure [47], in which starting from a non-orthogonal basis set $\{\varphi_k,\varphi_\alpha\}$ (φ_k and φ_α correspond to states of the isolated subsystems), the application of $(1+S)^{-\frac{1}{2}}$, where S is the overlap matrix produces the desired orthonormal basis set $\{\Phi_k,\Phi_\alpha\}$. A complete orthogonalization between the adsorbate and substrate original states is out of question and therefore it is natural to appeal to an expansion in terms of the overlap $S_{\alpha k}$ matrix elements. Thus, by using a lineal combination of atomic orbitals (LCAO) for the substrate states and performing a mean-field approximation on the many-body interaction terms, one arrives to the orbital energies E^σ_α and hopping term $T^\sigma_{\alpha k}$ (see Ref. [44] for a more detailed description):

$$E^\sigma_\alpha = \epsilon^0_\alpha + U^0_{\alpha\alpha}\langle n_{\alpha-\sigma}\rangle - \sum_{R_S} T^{Z_S}_{\alpha\alpha} + \sum_{i,R_S}(J^0_{\alpha i}\langle n_{i-\sigma}\rangle + G_{\alpha i}\langle n_{i\sigma}\rangle) - \sum_{i,R_S} S_{\alpha i}T^\sigma_{\alpha i} + \frac{1}{4}\sum_{i,R_S} S^2_{\alpha i}\Delta E^\sigma_{\alpha i} \quad (14)$$

with

$$T^\sigma_{\alpha k} \simeq \sum_{i,R_S} c^k_{iR_S}T^\sigma_{i\alpha} \quad (15)$$

The indexes i and j run over the orbitals of the substrate atoms located at the position vector $\vec{R}_S$; and the $c^k_{iR_S}$ are the coefficients of the LCAO expansion of the solid k-states. The $(\epsilon^0_\alpha - \sum_{R_S} T^{Z_S}_{\alpha\alpha})$ term accounts for the one electron contributions (kinetic energy and electron–nuclei interactions); $U^0_{\alpha\alpha}$ is the intra-atomic coulomb repulsion term, while $J^0_{\alpha i}$ and $G_{\alpha i}$ are respectively the direct and exchange coulomb integrals, all of them calculated by using the non-orthogonal atomic basis set. The $\Delta E^\sigma_{\alpha i}$ corresponds to the difference between the projectile and surface atom energy terms. Eq. (15) indicates that the atom–surface hopping is defined only with functions orthogonalized in each dimeric space $(\vec{R},\vec{R}_S)$. The $T^\sigma_{\alpha i}$ includes the hopping contributions due to the two-electron terms within a mean-field approximation. As the core states (l) of the substrate are assumed to be strongly localized, the corresponding hopping integrals $T_{\alpha l}(t)$ are the atomic ones between the α-orbital of the projectile and the 1s, 2s and 2p-orbitals of the target atom.

All the one and two-electron atomic integrals required to calculate Eqs. (14) and (15) are obtained from a Quantum Chemistry code,[1] calculated with the Gaussian atomic basis orbitals given by Huzinaga [48].

The $E^\sigma_\alpha(\vec{R})$ and $T^\sigma_{\alpha i}(\vec{R},\vec{R}_S)$ quantities are obtained from the static atom–surface interaction by taking the average occupations of the projectile and surface atoms frozen at their values in the non-interacting limit. That is, the $\langle n_{i\sigma}\rangle$ for the surface atoms are calculated consistently with the local density of states of the isolated, although infinitely extended surface. $\langle n_{\alpha\sigma}\rangle$ corresponds to the initial charge-state configuration of the projectile. For a neutral incoming projectile H^0 ($\langle n_{\alpha\uparrow}\rangle = 1$, $\langle n_{\alpha\downarrow}\rangle = 0$), the active state corresponds to the affinity level $E^\downarrow_\alpha(\vec{R})$ when the H^- formation is analyzed. In this case the expressions for $E^\downarrow_\alpha(\vec{R})$ and $T^\downarrow_{\alpha i}(\vec{R},\vec{R}_S)$ required for the spin-less description are determined by taking $\langle n_{\alpha\uparrow}\rangle = 1$ and $\langle n_{\alpha\downarrow}\rangle = 0$.

The energy level $E_\alpha(\vec{R})$ calculated in this way takes into account only short-range interactions between the projectile with the nearly surface atoms 'seen' along its trajectory. The effects of long-range interactions can be considered by the introduction of an image potential. For large normal distances (z) to the surface ($z \geqslant z_0 \simeq 8$ bohr accordingly to studies performed in the Al surface case [49]), the shift of the affinity level of the projectile in front of the semiconductor surface can be taken into consideration by using the expression [50]:

$$T_{\mathrm{im}}(z) = -\frac{\varepsilon(\omega)-1}{\varepsilon(\omega)+1}\times\frac{1}{4z} \quad (16)$$

where $\varepsilon(\omega)$ is expected to be adequately described by the static dielectric constant $\varepsilon(0)$ in the case of low projectile velocities. At large velocities the projectile does not have enough time to respond to the field of the moving charge.

[1] This calculation was performed using the commercial program GAUSSIAN98.

Thus, in this case it seems more appropriate to use the 'effective' dielectric constant given by the 'optical' value $\varepsilon(\infty)$ [50]. For surface, $\varepsilon(\infty)=1.1$ and $\varepsilon(0)=11.9$ [51]. Subsequently the matching procedure of joining both regions is performed, as this has proved to be successful in previous works [19,26,42]. Under this assumption the energy level as a function of the projectile–surface distance $\overline{R}$ is then taken as [49]

$$E_\alpha(\overline{R})=\begin{cases}\epsilon_\alpha(\overline{R})-\epsilon_\alpha(\overline{R}_0)+\epsilon_\infty+T_{\rm im}(z_0) & z<z_0\\ \epsilon_\infty+T_{\rm im}(z) & z\geqslant z_0\end{cases} \tag{17}$$

In the case of H^- formation $\epsilon^{\downarrow}_\infty=-0.75$ eV. In this form the energy level obtained within the mean field calculation is shifted to match smoothly the correct asymptotic behavior that includes the effect of the long range interactions (the $-\epsilon_\alpha(\overline{R}_0)+\epsilon_\infty$ term accounts for the correct location of the affinity level).

In addition to the dynamical aspects of the charge transfer process, it is necessary to account for the shift of the projectile state as well as for the change in momentum of the electron as it 'jumps' either to or from a moving center. The usual procedure to take into account these effects is to include the asymptotic behavior of the projectile wave function (φ'_α) as seen from the surface reference frame in the form:

$$\varphi'_\alpha(\bar r,t)=\exp(i\bar v\cdot\bar r)\varphi_\alpha(\bar r-\overline{R}(t))\exp\{-i[E_\alpha(\overline{R})+v^2/2]t\} \tag{18}$$

where $\varphi_\alpha(\bar r-\overline{R}(t))$ is the static wave function and $\bar v$ is the projectile velocity. This expression, that is assumed to be valid at any $\overline{R}$ implies the electron-translation factor [52] that should be included in the calculation of the energy level and hopping terms for an appropriate description of the charge exchange. By decomposing the wave-vector $\bar k$ corresponding to the substrate states into its parallel and perpendicular components $\bar k=(k_\parallel,k_\perp)$ and considering Eqs. (11)–(13) one can see that only the parallel component of the projectile velocity $\bar v_\parallel$ enters into the energy shift of the surface states while matrix elements of the coupling terms depend on both $\bar v_\parallel$ (parallel) and $\bar v_{\rm p}$ (perpendicular) [41]. In a complete and correct calculation of the self-energies, a matter of consistency requires $\bar v_\parallel$ should be fully included. This represents a formidable task particularly when contributions of many atoms of the substrate along the projectile trajectory are involved. As an approximation, we will neglect any explicit dependence on $\bar v_\parallel$ in the calculation of the self-energies, while only the energy phase depending on $\bar v_p$ will be retained. This is equivalent to consider the atomic energy level position changes as

$$E_\alpha[\overline{R}(t)]\rightarrow E_\alpha[\overline{R}(t)]+v_p^2/2 \tag{19}$$

As stated in Section 1 the main results of the present paper are related with a exhaustive calculation of the short range interactions between the projectile and the surface, by including a realistic description of the electronic structure and surface topography. Results including the approximated treatments of long range interaction and translation factor are also presented, but only to infer about the relative importance of these two effects. By the other hand, as in the Al surface case it is found that both effects have to be introduced together because of a detailed balance between them [49].

2.4. Self-energies and projectile's trajectory

Returning to the expressions (11)–(13) and using the expansion LCAO (Eq. (15)) for the hopping term $T^\sigma_{\alpha k}$, one can write the self-energies defined in terms of the local density of states of the Si(1 0 0)2 × 1 (or Si(1 1 1)7 × 7) surface and the atomic H–Si hopping integrals:

$$\Sigma^{\rm A}_V(t,t_1)=i\Theta(t_1-t)\sum_{i,j}\int_{-\infty}^{\infty}d\epsilon\rho_{ij}(\epsilon)T^*_{\alpha i}(t)T_{j\alpha}(t_1)\times\exp[-i\epsilon(t-t_1)] \tag{20}$$

$$\Omega_V(t,t_1)=-i\sum_{i,j}\int_{-\infty}^{\infty}d\epsilon\rho_{ij}(\epsilon)T^*_{\alpha i}(\overline{R}(t)-\overline{R}_S)T_{j\alpha}(\overline{R}(t_1)-\overline{R}_S)\times\exp[-i\epsilon(t-t_1)](1-2f(\epsilon)) \tag{21}$$

where $f(\epsilon)$ is the Fermi-distribution function, and $\rho_{ij}(\epsilon)$ is the local-partial density of states defined as

$$\rho_{ij}(\epsilon)=\sum_k c^{k*}_{i,R_S}c^{k*}_{j,R_S}\delta(\epsilon-\epsilon_k) \tag{22}$$

Concerning with the collision geometry arrangement, the *incoming* and *outgoing* trajectories of the H projectile are roughly simulated by straight lines with the correct incidence and exit angles with reference to the surface. The incoming projectile follows a trajectory given by the incident angle $\theta_{\rm in}$ and directed towards the surface scatterer atom, while the outgoing scattered particles H^- follows a trajectory given by $\theta_{\rm out}$ (the trajectory is assumed to occur in the x–z plane, where the z-axis is perpendicular to the surface). Thus, $\theta_{\rm out}=\delta_{\rm SC}-\theta_{\rm in}$, where $\delta_{\rm SC}=38°$ corresponds to the fixed scattering angle. For a given incoming kinetic energy, the distance of closest approach $R_{\rm min}$ is previously obtained from the interaction energy between H^0 and one Si atom, with values 0.225 and 0.09 a.u. for $E_{\rm kinetic}=1$ and $E_{\rm kinetic}=4$ keV, respectively. In this case, the laboratory frame is assumed to be coincident with the center of mass of the H^0–Si system. The $(x_{\rm min},z_{\rm min})$ coordinates of $R_{\rm min}$ are determined by using the usual concepts of two-body scattering theory [53]. Thus

$$\begin{aligned}\rho_{\rm min}&=-R_{\rm min}\cos(\psi+\theta_{\rm in})\\ x_0&=\rho_{\rm min}\cos\beta\\ y_0&=\rho_{\rm min}\sin\beta\\ z_0&=R_{\rm min}\sin(\psi+\theta_{\rm in})\end{aligned} \tag{23}$$

where β corresponding to azimuthal angle, and $\psi=(\pi-\delta_{\rm SC})/2$.

It is worth pointing out here that the target atom recoil is neglected. Within our calculation, the projectile energy

loss is accounted for by considering different ion velocities along the *incoming* and the *outgoing* parts of the trajectory.

2.5. Reconstructed Si(100)2 × 1 and Si(111)7 × 7 surfaces: partial and local density of states

The structure relaxations have been optimized by the use of an ab initio code (FIREBALL96) [43]. This is based on density functional theory (DFT), using a local density approximation (LDA) for the exchange-correlation functional for a localized atomic orbital basis. In Fig. 1(a) and (b) one can observe schematically the surface structure corresponding to the 2×1 [54,55] and 7×7 [56,54] reconstructed Si(100) and Si(111) surfaces, respectively. The local and partial density of states calculated for the infinitely extended surface and projected onto the different surface atoms correspond to these geometric arrangements. The depths of the slabs, ranging from about 20 and 14 a.u. have been selected as to have always 'bulk' atoms within the 'interaction sphere' of the projectile at its closest approach to the scatterer center. Possible trajectories are taken along the 'trenches' seen in the figures for both structures, and the labelled atoms in Fig. 1(a) and (b) are the selected scatterer centers as an attempt to account for the 'averaging effect' of the experimental situation.

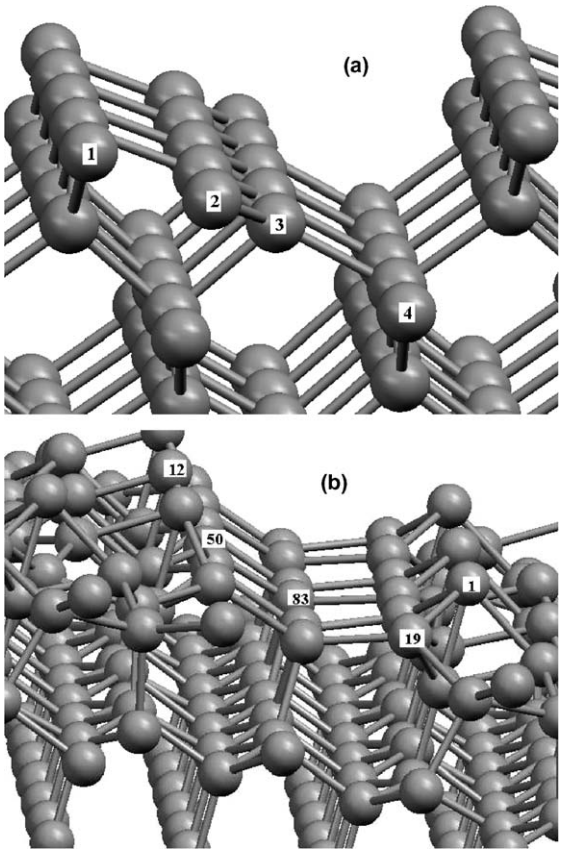

Fig. 1. Schematic view of the surface structure corresponding to the 2×1 (a) and 7×7 (b) reconstructed Si(100) and Si(111) surfaces, respectively.

3. Results and discussion

In Fig. 2 the affinity energy level of the projectile $E_a(\overline{R})$, for $\theta_{out}=12°$, is plotted as a function of the normal distance to the surface. Negative (positive) values for z correspond to the incoming (outgoing) trajectory. In this case the atom labelled 1 in Fig. 1(b) is the surface scattering center. The local density of states (DOS) for this atom 1 calculated by using the FIREBALL96 code is also shown in Fig. 2. One can observe the presence of narrow bands of surface-like states near to the Fermi level. To infer about the effects of these narrow peaks in the density of states on the charge transfer processes, we performed calculations for normal trajectories with respect to the surface including only the interaction of the projectile with the scatterer atom. The incidence velocities are taken as those corresponding to the perpendicular component of the velocity according to the scattering geometry under study [$v_{p,in(out)}=v\sin\theta_{in,(out)}$]. In this kind of calculation the v_p velocity component is the only one involved. Thus, any difference found between results at the two kinetic energies (1 and 4 keV) when analyzing the ion fraction as a function of $v_{p,out}$ can only be due to memory effects during the incoming trajectory. In Fig. 3 the ion fractions calculated in this way for the Si(100)2 × 1 surface, for scatterer atoms labelled as 1 and 2 in Fig. 1(a), are shown. In Figs. 4 and 5 the results for the Si(111)7 × 7 for the scatterer atoms labelled as 1, 19, 12 and 50 in Fig. 1(b) are presented. The corresponding local DOS for each surface atom is also shown. Results obtained from similar calculations but omitting core levels of the target atom are also included. For large exit v_p, it can be seen that for scatterer with pronounced narrow bands in the DOS near the Fermi energy [atoms 1 and 12 of the Si(111)7 × 7 surface] the incoming trajectory becomes very important in defining the final charge state. By comparing these with results obtained by ignoring the surface core states, we can infer that the

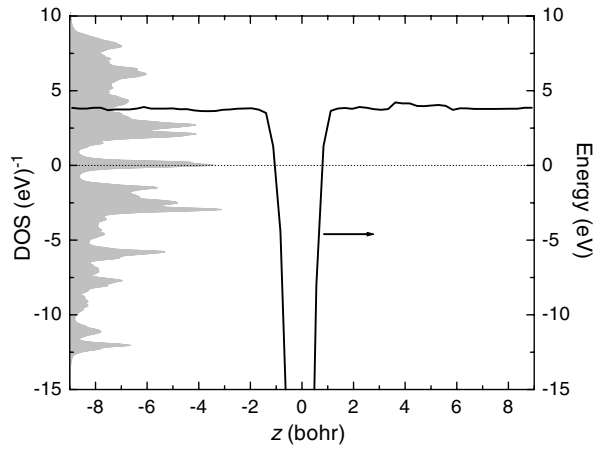

Fig. 2. Affinity energy level of the projectile $E_a(\overline{R})$, for $\theta_{out}=12°$, as a function of the normal distance to the surface. The surface scatterer is the atom 1 in Si(111)7 × 7. The local DOS for this atom (shadowed) is also shown.

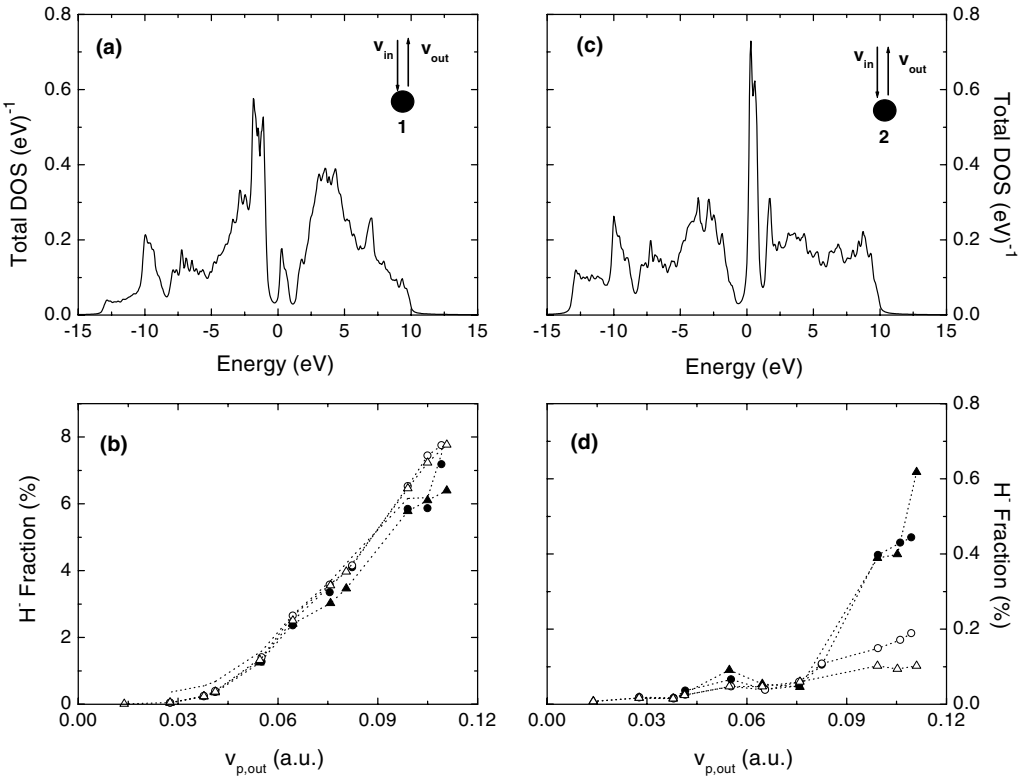

Fig. 3. (a) The local DOS of the scatterer atom 1 for the Si(1 0 0)2 × 1 surface. (b) Negative ion fractions obtained for normal incidence with respect to the surface, including only the interaction of the projectile with the scatterer atom 1. Full (empty) symbols correspond to the calculation with (without) the core levels of the target atom. Circles are for 4 keV while triangles are for 1 keV. (c) and (d) the same as (a) and (b) for atom 2 as the scattering center in Si(1 0 0)2 × 1 surface.

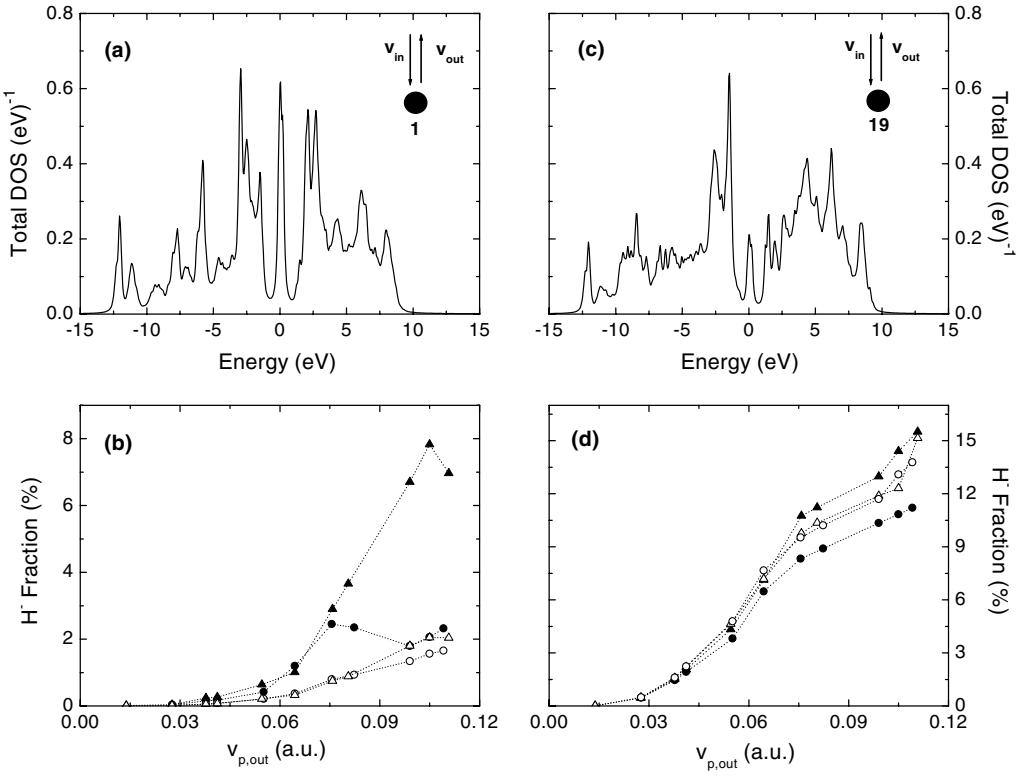

Fig. 4. The same as in Fig. 3: (a), (b) for atom 1; and (c), (d) for atom 19 as scattering centers in the Si(1 1 1)7 × 7 surface.

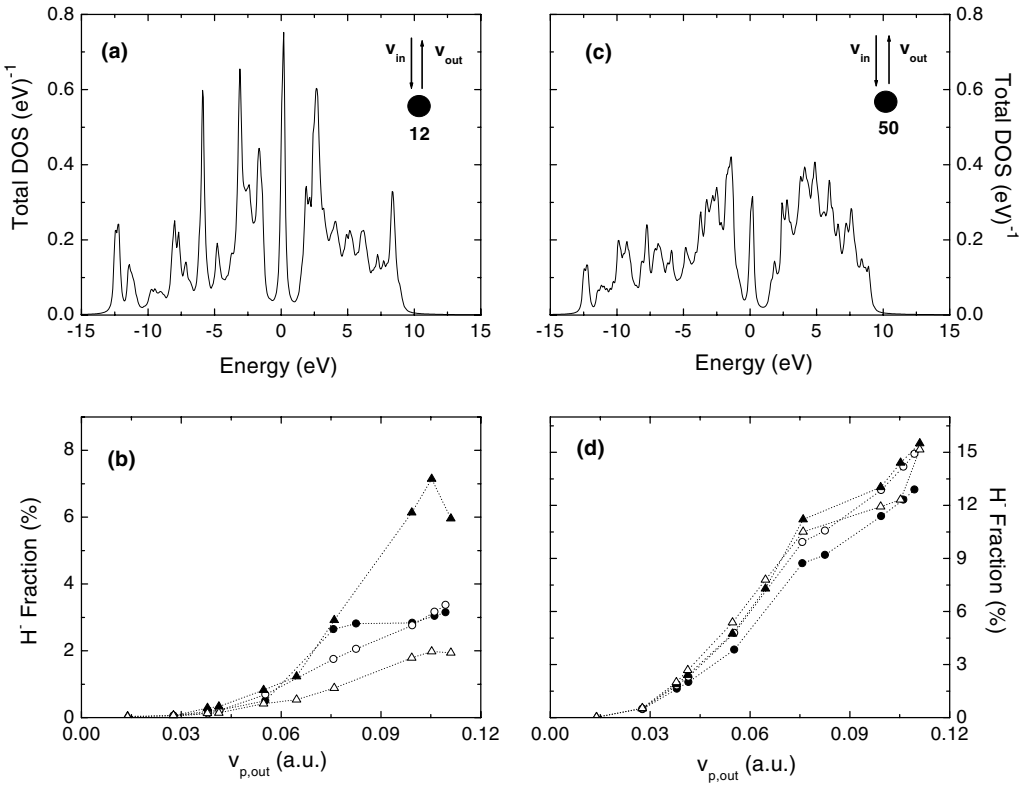

Fig. 5. As in Fig. 4: (a), (b) for atom 12; and (c), (d) for atom 50 as scattering-centers in the Si(1 1 1)7 × 7 surface.

responsible of this memory effect is the projectile level shift caused by the interaction with these deep levels, particularly when confronted with a valence band also exhibiting narrow surface state structures. This effect is expected to become more pronounced whenever the ion enters slowly towards the scatterer as to allow for the formation of quasi-molecular states, followed by a rapid departure from the surface neighborhood in the exit part of the trajectory. The analysis of the other scattering center situations in both surfaces [Si(1 0 0)2 × 1 and Si(1 1 1)7 × 7] leads to similar conclusions: the incoming trajectory memory and the close collision region are both important to define the ion fractions whenever a significative structure of narrow bands in the local DOS is present. By contrast, if the DOS reflects wide band features, the final projectile state of charge is defined by the outgoing part of the trajectory and not very close to the surface, where the interaction with inner states becomes important. That is the case of the atom 1 of the Si(1 0 0)2 × 1 surface. In a real experimental situation the projectile interacts with many surface atoms along its trajectory. Also, one expects that some sort of averaging from different scattering centers will be present in the overall signal response. Consequently, in order to understand the complexities of the atom–surface collision we will analyze first the collision with individual scatterer atoms. In Fig. 6 the negative ion fractions calculated as a function of the outgoing v_p are shown for the 1 and 4 keV kinetic energies. These correspond to the 1 and 2 scatterer atoms in the Si(1 0 0)2 × 1 surface and 1 and 19 for the Si(1 1 1)7 × 7 case. Data obtained by Maazouz et al. [39] are also included in this figure. It is observed in Fig. 6 that the ion fraction behavior for 4 keV are less dependent on the scattering situation than for the 1 keV case. One can also observe that our results follow the general trends of the experiment for the outermost scatterer atoms in both reconstructed surfaces (atom 1), being independent on the energy at large values of the outgoing v_p. By taking into account that the projectile is interacting with all surface atoms seen along its trajectory, one expects a blurring of the effects caused by the sharp narrow band features in a sort of trajectory averaged response to the different kind of substrate atoms that participate. This could be an explanation to the observed behavior, although in the case of the other scatterer centers in both Si surfaces, an energy dependence is present along the whole range of outgoing v_p, suggesting a strong influence of the surface region over which the projectile is travelling. The calculation was repeated by omitting the Si core states. We found no effect due to these states when many atoms of the surface are involved in the interaction. The parallel component of the outgoing velocity is possibly the responsible of the difference between the two energies, because one expects for low v_p, that the smaller values of the parallel component in the case of 1 keV (varying from 0.2 to 0.166 a.u.) allow for a better discrimination of the electronic and atomic surface details. The same is concluded in H^- formation on Ag(1 1 1) and Cu(1 1 1): the electron needs a finite time to move into the metal and explore the *bulk* band structure; then if the col-

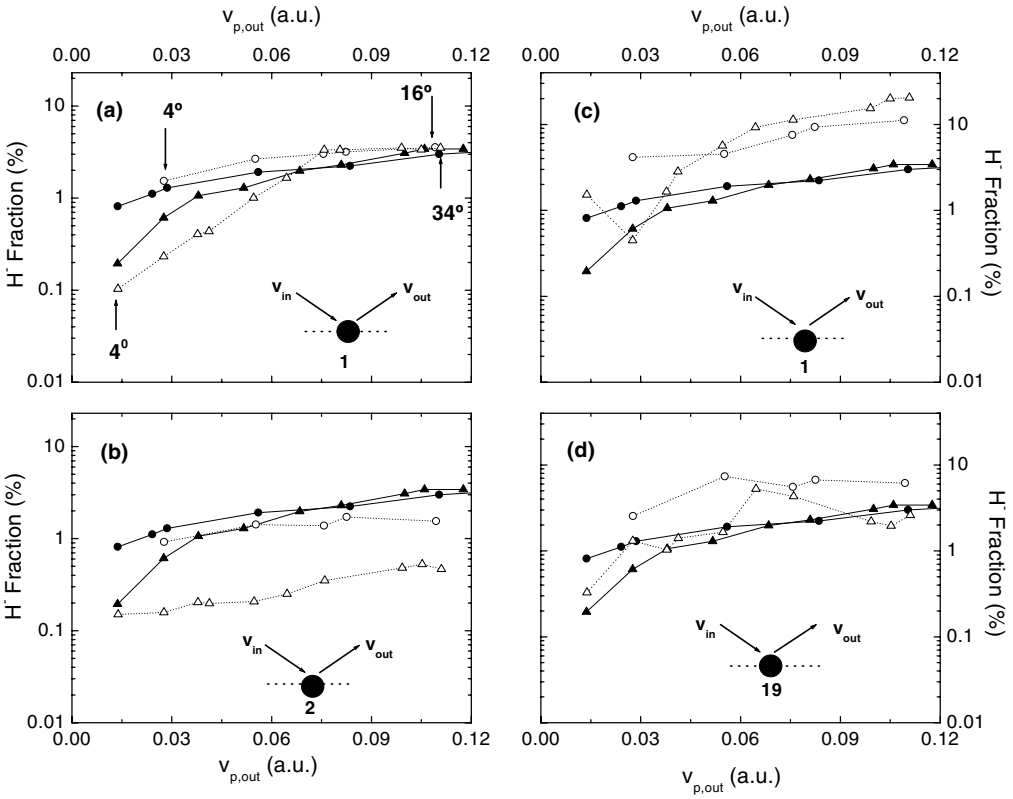

Fig. 6. Negative ion fractions as a function of the outgoing perpendicular velocity. (a) Scatterer atom 1 for Si(1 0 0)2 × 1; (b) scatterer atom 2 for Si(1 0 0)2 × 1; (c) scatterer atom 1 for Si(1 1 1)7 × 7; (d) scatterer atom 19 for Si(1 1 1)7 × 7. Full symbols correspond to the experimental data. Empty symbols to theoretical results. Circles are for calculations at 4 keV and triangles for 1 keV.

lision is fast enough, the electron has not time to probe the surface properties and the resonant process has the jellium characteristics [30,31].

The calculated ion fractions as a function of the exit angle for the two incoming kinetic energies, and for all different scattering centers lying along the 'trenches' shown in Fig. 1(a) and (b) for both structures, are shown in Figs. 7 and 8. Again, less dispersion in the ion fractions is obtained for the 4 keV case. The marked oscillations observed in the case of Si(1 1 1)7 × 7 can be due to the more pronounced narrow band structures in the DOS of this reconstructed surface, that lead to non-resonant processes like the ones occurring in gas phase collisions [39]. The average values for each case are also shown in Figs. 7 and 8. It can be observed that the averaged ion fractions exhibit a smooth dependence on the exit angle when compared with those obtained for individual scatterer atoms. This result is more striking for the Si(1 1 1)7 × 7 surface. In Fig. 9 the averaged ion fractions as a function of v_p and also as a function of the exit angle for Si(1 0 0)2 × 1 surface, are compared with the experimental data obtained at 1 and 4 keV. The same comparison for the Si(1 1 1)7 × 7 is presented in Fig. 10. In both cases the overall qualitative behavior of the experiment is reproduced. These results suggest again that a blurring of the effects caused by the sharp narrow band features occurs as the result of the averaged individual response due to the different kind of scattering centers. In

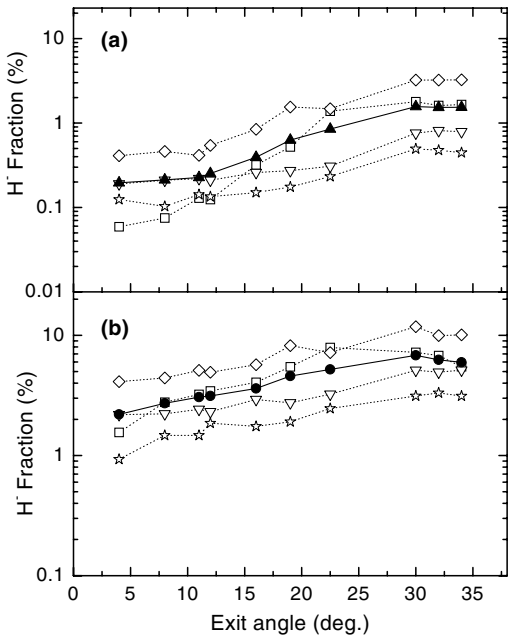

Fig. 7. Negative ion fraction as a function of exit angle in the Si(1 0 0)2 × 1 surface, (a) 1 keV; (b) 4 keV. Full symbols correspond to theoretical results averaged over all scattering centers, circles for 4 keV and triangles for 1 keV. Squares are for atom 1; stars for atom 2; diamonds for atom 3 and down triangles for atom 4 as scatterer centers, respectively.

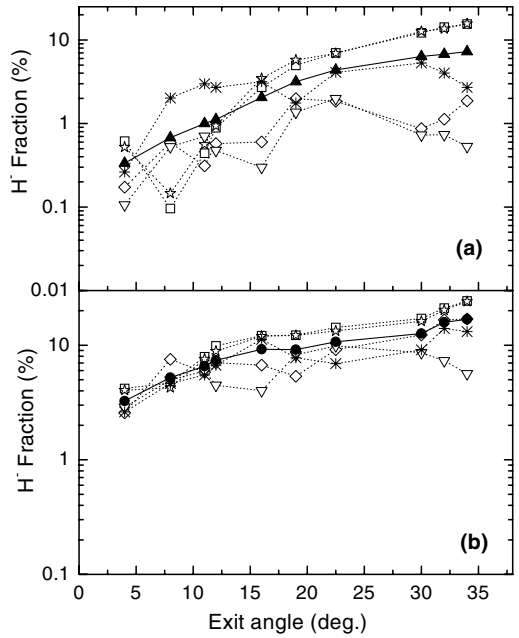

Fig. 8. As in Fig. 7 for Si(1 1 1)7 × 7 surface. Squares correspond to atom 1; stars to atom 12; diamonds to atom 19; down triangles to atom 50 and crosses to atom 83 as scattering sites, respectively.

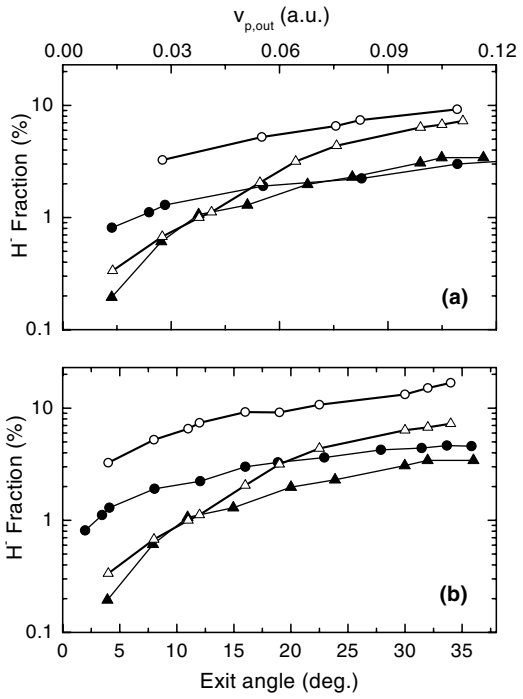

Fig. 10. The same as in Fig. 9 to Si(1 1 1)7 × 7 surface.

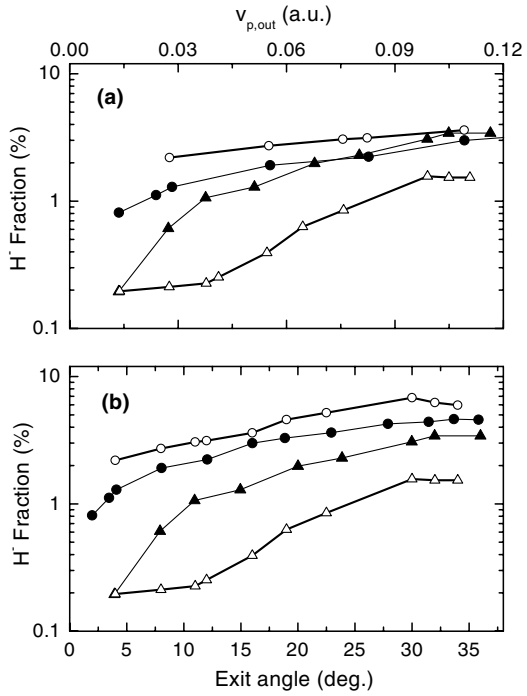

Fig. 9. Si(1 0 0)2 × 1 (a) Negative ion fractions as a function of the outgoing perpendicular velocity. Full symbols correspond to the experimental data. Empty symbols to the averaged theoretical results omitting image potential and translation factor. Dots are for 4 keV and triangles for 1 keV. (b) As in (a) but as a function of the exit angle.

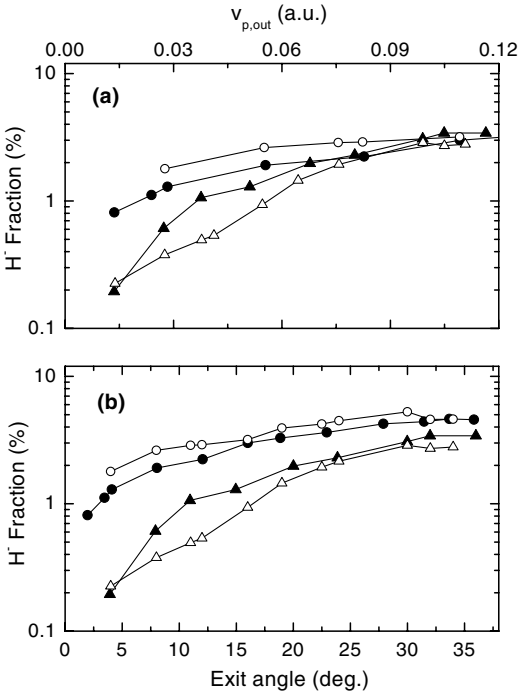

Fig. 11. Si(1 0 0)2 × 1 (a) Negative ion fractions as a function of the outgoing perpendicular velocity. Full symbols correspond to the experimental data. Empty symbols to the averaged theoretical results including image potential and translation factor. Dots are for 4 keV and triangles for 1 keV. (b) As in (a) but as a function of the exit angle.

Figs. 11 and 12 results obtained by including translation factor and the image potential are shown. The last one has been taken as $T_{\mathrm{im}}(z) = -\frac{\varepsilon-1}{\varepsilon+1} \times \frac{1}{4z}$, with $\varepsilon(\infty) = 1.1$ for the case of incoming ions of 4 keV and $\varepsilon(0) = 11.9$ for the 1 keV case. For Si(1 0 0)2 × 1 surface, an improvement in the agreement with the experiment is observed. However, it must be stressed that the inclusion of both of these effects do not change the basics tendencies.

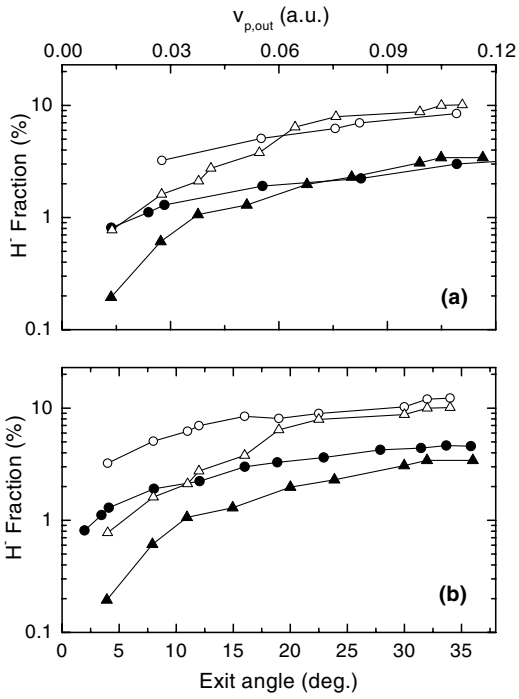

Fig. 12. The same as in Fig. 11 to Si(1 1 1)7 × 7 surface.

On the other hand, in the experimental study some amorphization of the Si(1 1 1)7 × 7 sample may occur. Then, neither the Si(1 1 1)7 × 7 nor the Si(1 0 0)2 × 1 surfaces analyzed in this work correspond exactly to the experimental situation. According to our results, the general qualitative behavior of the measured ion fraction is quite independent of the detailed features of the surface because the averaging response effects present in this range of angles and incoming energies. For either large exit angles or outgoing v_p the ion fraction becomes independent on the energy, while for large dwelling times in front of the surface the parallel component of the velocity, closely related to the projectile flying time along the surface, also determines the ion fraction behavior. Nevertheless for each individual scatterer atom the charge transfer process is strongly dependent on the surface region seen by the projectile along its trajectory. We found that the final averaged response of the surface to the ion beam is not very different when going from a Si to an Al surface [49].

A neutral atom as the initial charge condition has been considered in this whole analysis of the final negative ion fraction of hydrogen. The same results were obtained when performing the calculation by considering a negative ion as the incoming particle. This indicates the rapid and efficient neutralization of hydrogen occurring along the incoming trajectory.

4. Conclusions

We have performed a calculation of the negative ion fractions based on a detailed description of the interaction parameters for the system H–Si, and also by using a realistic density of states for the two reconstructed surfaces Si(1 0 0)2 × 1 and Si(1 1 1)7 × 7. By including the interaction of the ion projectile with many target atoms seen during its trajectory and averaging over a variety of scatterer centers occurring in the experimental situation, we obtained a smooth dependence with the exit angle that does not reflect the specific details of the local DOS and the surface topography. Averaging effects lead to similar ion fraction behaviors for the two analyzed surfaces. Also, in this range of angles and energies a similar behavior to that found for the Al surface was obtained. Oscillations were observed in the ion fraction as function of the exit angle for individual scattering centers, being more striking in the case of pronounced narrow band structures in the surface DOS (Si(1 1 1)7 × 7). This result suggests that non-resonant processes of charge exchange between localized states as either in gas phase collisions, or in the case of insulator surfaces [57] may also be of significance.

For large values of the outgoing v_p (large exit angles), the ion fraction seems to be almost independent on the incoming energy, while in the opposite cases where the projectile spends longer times in contact with the surface, the effect of the parallel component of the velocity has an increasing importance. It is observed that the fine details of the surface are 'better captured' as the parallel velocity component becomes smaller. This effect is independent of the image potential used to account for the long range interactions.

Acknowledgements

This work was supported by Grants (PIP) No. 2833 and (PEI) No. 6173 from CONICET, and (CAI + D) No. 6-1-76 from UNL, Argentina. E.A.G. acknowledges partial support from Fundación Antorchas, Argentina (No. A13927-17). P.G.B. acknowledges to Fundación Antorchas and ANPCyT by Grants 14248-128 and 03-11769, respectively. E.A.G., P.G.B., M.C.G. and E.C.G. are research staff members of CONICET.

References

[1] R. Souda, T. Aizawa, C. Oshima, S. Otani, Y. Ishizawa, Phys. Rev. B 40 (1839) 4119.
[2] R. Souda, K. Yamamoto, W. Hayami, T. Aizawa, Y. Ishizawa, Phys. Rev. B 51 (1995) 4463.
[3] M. Maazouz, G. Borisov, V.A. Esaulov, J.P. Gauyacq, L. Guillemot, S. Lacombe, D. Teillet-Billy, Phys. Rev. B 55 (1997) 13869.
[4] M. Maazouz, S. Usteze, L. Guillemot, V.A. Esaulov, Surf. Sci. 409 (1998) 189.
[5] A. Blandin, A. Nourtier, D.W. Hone, J. Phys. (París) 37 (1976) 369.
[6] R. Brako, D.M. Newns, Surf. Sci. 108 (1981) 253.
[7] J.J.C. Geerlings, J. Los, J.P. Gauyacq, N.M. Temme, Surf. Sci. 172 (1996) 257.
[8] H. Saho, D.C. Langreth, P. Nordlander, Phys. Rev. B 49 (1994) 13929.
[9] Evelina A. García, E.C. Goldberg, M.C.G. Passeggi, Surf. Sci. 325 (1995) 311.
[10] Evelina A. García, P.G. Bolcatto, E.C. Goldberg, Phys. Rev. B 52 (1995) 16924.

[11] R.L. Erickson, D.P. Smith, Phys. Rev. Lett. 34 (1975) 29.
[12] J.W. Rabalais, J.N. Chen, R. Kumar, Phys. Rev. Lett. 55 (1985) 1124.
[13] R. Souda, M. Aono, C. Oshima, S. Otani, Y. Ishizawa, Nucl. Instr. Meth. Phys. Res. B 15 (1986) 138.
[14] M.L. Yu, N.D. Lang, Phys. Rev. Lett. 50 (1983) 127.
[15] H. Niehus, K. Mann, B.N. Elohidge, M.L. Yu, J. Vac. Sci. Technol. A 6 (3) (1998) 625.
[16] D.C. Jacobs, J.R. Morris, J.S. Martin, J.N. Greeley, Surf. Sci. 330 (1995) 323.
[17] L. Houssiau, J.W. Rabalais, J. Wolfgang, P. Nordlander, J. Chem. Phys. 110 (1999) 8139.
[18] D.J. O'Connor, R.J. Mac Donald, Surf. Sci. Lett. 100 (1980) L495.
[19] H. Verbeek, W. Eckstein, R.S. Bhattacharya, Surf. Sci. 95 (1980) 330.
[20] V.A. Kurnaev, N.N. Koborov, G.I. Zhabrev, O.V. Zabeida, Nucl. Instr. Meth. Phys. Res. B 78 (1993) 63.
[21] D.V. Ledyankin, I. Urazgildin, V. Yurasova, Sov. Phys. JETP 67 (1988) 2442.
[22] J.H. Rechtien, U. Imke, K.J. Snowdon, P.H.F. Reijnen, P.J. van den Hoek, A.W. Kleyn, Surf. Sci. 227 (1990) 35.
[23] B. Hird, R.A. Armstrong, P. Gauthier, Surf. Sci. 292 (1993) 305.
[24] R. Souda, E. Asari, H. Kawanowa, T. Suzuki, S. Otani, Surf. Sci. 421 (1999) 89.
[25] C.T. Rettner, Phys. Rev. Lett. 69 (1992) 383.
[26] C.A. Staldi, A. Bianco, S. Modesti, E. Tosatti, Phys. Rev. Lett. 68 (1992) 90.
[27] K. Sumitomo, T. Kobayashi, F. Shoji, K. Oura, I. Katayama, Phys. Rev. Lett. 66 (1991) 1193.
[28] J.R. Hiskes, P.J. Schneider, Phys. Rev. B 23 (1981) 949.
[29] W. Eckstein, F.E.P. Matshke, Phys. Rev. B 14 (1976) 3231.
[30] L. Guillemot, V.A. Esaulov, Phys. Rev. Lett. 82 (1999) 4552.
[31] A.G. Borisov, A.K. Kazansky, J.P. Gauyacq, Phys. Rev. B 59 (1999) 10935.
[32] R. Souda, T. Aizawa, W. Hayami, S. Otani, Y. Ishizawa, Phys. Rev. B 42 (1990) 7761.
[33] R. Souda, W. Hayami, T. Aizawa, Y. Ishizawa, Phys. Rev. B 43 (1991) 10062.
[34] R. Souda, T. Suzuki, K. Yamamoto, Surf. Sci. 397 (1998) 63.
[35] F. Wyputta, R. Zimny, H. Winter, Nucl. Instr. Meth. Phys. Res. B 58 (1991) 379.
[36] H. Nienhaus, R. Zimny, H. Winter, Radiat. Eff. Defects Solids 109 (1989) 1.
[37] R. Zimny, H. Nienhaus, H. Winter, Nucl. Instr. Meth. Phys. Res. B 48 (1990) 361.
[38] A.G. Borisov, D. Teillet-Billy, J.P. Gauyacq, Phys. Rev. Lett. 68 (1991) 2842;
A.G. Borisov, D. Teillet-Billy, J.P. Gauyacq, Surf. Sci. 278 (1992) 99.
[39] M. Maazouz, L. Guillemot, V.A. Esaulov, D.J. O'Connor, Surf. Sci. 398 (1998) 49.
[40] M. Maazouz, A. Borisov, V.A. Esaulov, J.P. Gauyacq, L. Guillemot, S. Lacombe, D. Teillet-Billy, Surf. Sci. 364 (1996) L568.
[41] J. Merino, N. Lorente, F. Flores, M. Yu Gusev, Nucl. Instr. Meth. Phys. Res. B 125 (1997) 250, With reference to Eq. (17) in this paper, our proposal would have been to take $g_{k_\parallel}, \delta_\mu(\omega + \overline{k}_\parallel \cdot \overline{v} - v_\parallel^2/2)$ instead of using $g_{k_\parallel}, \delta_\mu(\omega + \overline{k}_\parallel \cdot \overline{v} - v^2/2)$.;
See also N. Lorente, J. Merino, F. Flores, M. Yu Gusev, Nucl Instr. Meth. Phys. Res. B 125 (1997) 277.
[42] J. Merino, N. Lorente, P. Pou, F. Flores, Phys. Rev. B 54 (1996) 10959.
[43] O.F. Sankey, D.J. Niklewski, Phys. Rev. B 40 (1989) 3979;
A.A. Demkov, J. Ortega, O.F. Sankey, M.P. Grumbach, Phys. Rev. B 52 (1995) 1618.
[44] P.G. Bolcatto, E.C. Goldberg, M.C.G. Passeggi, Phys. Rev. B 58 (1998) 5007.
[45] L.V. Keldysh, Zh. Eksp. Teor. Fiz. 47 (1964) 1515 [Sov. Phys. JETP 20 (1965) 1018].
[46] E.C. Goldberg, E.R. Gagliano, M.C.G. Passeggi, Phys. Rev. B 32 (1985) 4375.
[47] P.O. Lowdin, J. Chem. Phys. 18 (1950) 365.
[48] S. Huzinaga, J. Chem. Phys. 42 (1965) 1293;
S. Huzinaga, J. Andzelm, M. Klobukowski, E. Radzio-Andzelm, Y. Sakai, H. Tatewaki, in: S. Huzinaga (Ed.), Gaussian Basis Set for Molecular Calculations, Elsevier, Amsterdam, 1984.
[49] M.C. Torralba, P.G. Bolcatto, E.C. Goldberg, Phys. Rev. B 68 (2003) 075406.
[50] A.G. Borisov, V.A. Esaulov, J. Phys.: Condens. Matter 12 (2000) R177.
[51] G. Srinivasan, Phys. Rev. 178 (1969) 1244.
[52] J.B. Delos, Phys. Rev. A 23 (1981) 2301.
[53] H. Goldstein, in: Aguilar (Ed.), Classical Mechanics, Madrid, Spain, 1970.
[54] W. Mönch, in: Semiconductor Surfaces and Interfaces, Springer Series in Surface Science, vol. 26, Springer-Verlag, Berlin, Heidelberg, Germany, 1995.
[55] Andrew Zangwill, Physics at Surfaces, University Press, Cambridge, 1990.
[56] Guo-Xin Quian, D.J. Chadi, Phys. Rev. B 35 (1987) 1288.
[57] J.O. Lugo, E.C. Goldberg, E.A. Sánchez, O. Grizzi, Phys. Rev. B 72 (2005) 035432.